energies

MDPI

Article

Gas Permeability Evolution Mechanism and Comprehensive Gas Drainage Technology for Thin Coal Seam Mining

Fangtian Wang [1], Cun Zhang [2,3,*] and Ningning Liang [1]

1 State Key Laboratory of Coal Resources and Mine Safety, School of Mines, Key Laboratory of Deep Coal Resource Mining, Ministry of Education of China, China University of Mining and Technology, Xuzhou 221116, China; wangfangtian111@cumt.edu.cn (F.W.); liangning@cumt.edu.cn (N.L.)

2 State Key Laboratory of Coal Resources and Mine Safety, College of Resources & Safety Engineering, China University of Mining and Technology (Beijing), Beijing 100083, China

3 Beijing Key Laboratory for Precise Mining of Intergrown Energy and Resources, China University of Mining and Technology (Beijing), Beijing 100083, China

* Correspondence: cumtzczlw@cumt.edu.cn; Tel.: +86-158-1019-4123

Received: 12 July 2017; Accepted: 8 September 2017; Published: 12 September 2017

Abstract: A thin coal seam mined as a protective coal seam above a gas outburst coal seam plays a central role in decreasing the degree of stress placed on a protected seam, thus increasing gas permeability levels and desorption capacities to dramatically eliminate gas outburst risk for the protected seam. However, when multiple layers of coal seams are present, stress-relieved gas from adjacent coal seams can cause a gas explosion. Thus, the post-drainage of gas from fractured and de-stressed strata should be applied. Comprehensive studies of gas permeability evolution mechanisms and gas seepage rules of protected seams close to protective seams that occur during protective seam mining must be carried out. Based on the case of the LongWall (LW) 23209 working face in the Hancheng coal mine, Shaanxi Province, this paper presents a seepage model developed through the FLAC3D software program (version 5.0, Itasca Consulting Group, Inc., Minneapolis, MI, USA) from which gas flow characteristics can be reflected by changes in rock mass permeability. A method involving theoretical analysis and numerical simulation was used to analyze stress relief and gas permeability evolution mechanisms present during broken rock mass compaction in a goaf. This process occurs over a reasonable amount of extraction time and in appropriate locations for comprehensive gas extraction technologies. In using this comprehensive gas drainage technological tool, the safe and efficient co-extraction of thin coal seams and gas resources can be realized, thus creating a favorable environment for the safe mining of coal and gas outburst seams.

Keywords: permeability evolution mechanism; protective seam mining; stress-relief; gas drainage technology; co-extraction of coal seam and gas resources

1. Introduction

In China, more than 50% of coal seams are high gas-containing coal seams, and high outburst mines account for 44% of all coal mines in the country [1–3]. With increases in coal mining depth and intensity levels, gas pressure and gas content levels will also increase significantly. Coal and gas outbursts have occurred more frequently, constituting a considerable threat to safe production in coal mines [4,5]. Instantaneous outburst is a complex phenomenon involving interactions between gas pressure, stress, and the physico-mechanical properties of the coal, and can occur under a variety of conditions [6]. As is shown in Figure 1, the percentage of gas-related accidents of all coal mine accidents remained at approximately 10% from 2005 to 2015. Meanwhile, the percentage of gas-related

deaths of all deaths occurring over the last decade has remained at approximately 30%. Gas accident hazards found in Chinese coal mines are thus very serious and have not been effectively controlled relative to other hazards. In addition, most coal seams in coal mines are low in permeability, low in pressure, low in gas saturation, and high in metamorphic degree levels, and 95% of high-gas and outburst mines coal seams present permeability levels of only 0.1×10^{-3}–1.0×10^{-3} mD, causing gas extraction efforts to have limited effects prior to coal seam mining [7–9]. Theoretical studies and field practice have shown that mining a protective seam can release stress and can improve the gas permeability of a coal seam, which can in turn enhance gas extraction and prevent coal and gas outbursts [10–14]. Thus, much research on the relationship between stress and permeability has been conducted [15–18]. However, stress-relief gas generated during protective coal seam mining mainly derives from a protective coal seam, a neighboring seam, or a distant overlying seam. The relaxing gas above flows in quantities to the working face and goaf, causing gas concentration limits to be exceeded and threatening safe conditions at the working face [19,20]. Thus, the comprehensive study of changes in gas permeability and gas seepage rules that apply during the mining of protective seams when a protected seam is located close to a protective seam must be carried out. Such research can also serve as a theoretical basis for mine gas extraction [21–24]. Regarding problems of high gas pressure, gas content, and stress levels related to deep mining, comprehensive methods including theoretical analyses of production data and field trials and numerical simulation methods—such as those of protective seam mining, hydrofracturing, and gas extraction—have been proposed as ways to reduce protected seam gas content and pressure [25–28]. Due to the limited thickness, low mining productivity, and low gas content of thin coal seams in the coal seam group, using thin coal seams as protective seams can improve the safety of mining coal seams [29,30].

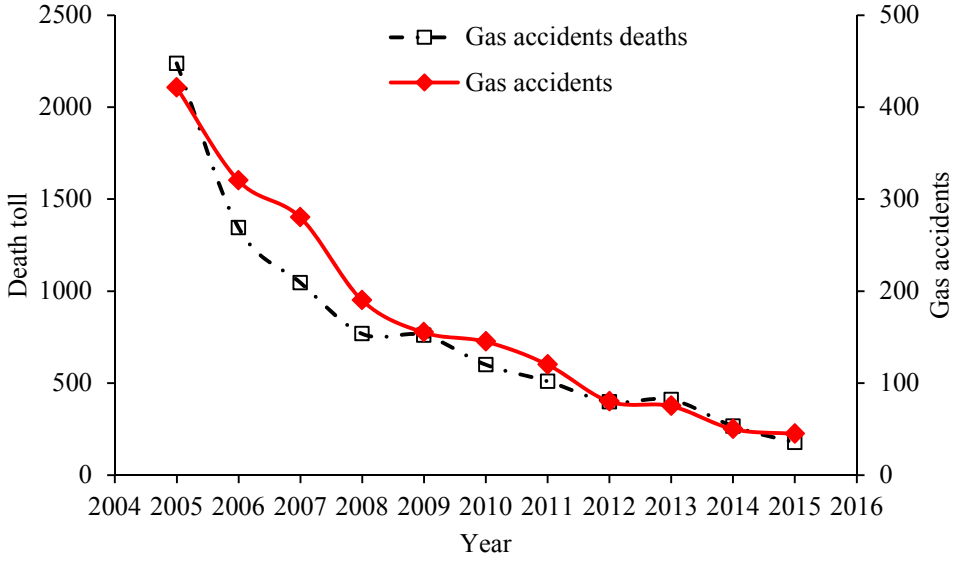

Figure 1. Gas accident statistics from 2005 to 2015 in China.

In combining methods of theoretical analysis, numerical simulation, and field application, this paper examines gas permeability evolution mechanisms and comprehensive gas drainage technologies involved during the thin coal seam mining of coal mines in Shaanxi Province, China. The in situ application results show that the safe mining of thin coal seams as protective seams and the simultaneous efficient drainage of gas resources from the protected coal seam has been realized, which should have favorable effects on the safe and efficient mining of coal and gas outburst seams, and which also supports greenhouse gas control.

2. Geological and Engineering Conditions

The LW23209 (LongWall23209) working face is located south of the Hancheng coal mine in Shaanxi Province, as shown in Figure 2. Its panel width and length are 140 m and 785 m, respectively. The #2 coal seam is identified as a non-outburst coal seam by the Coal Science Research Institute, Chongqing Branch, with gas content and average gas pressure levels lower than 6 m^3/t and 0.74 MPa, respectively.

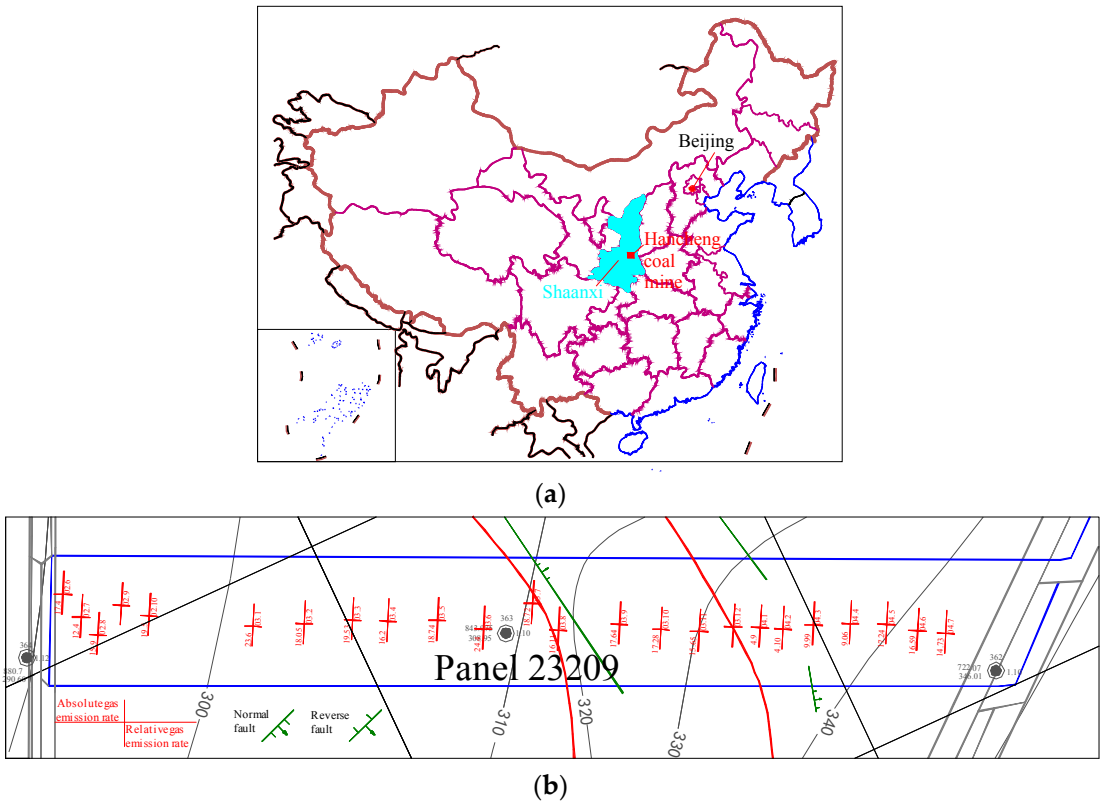

Figure 2. Location of the longwall panel LW23209, (**a**) location of Hancheng coal mine, (**b**) a plane view of the longwall panel LW23209.

The LW23209 working face of the #2 coal seam has a simple geological structure with an average seam thickness of 1.0 m. The average buried depth of the working face is 552 m, and gas pressure levels reach 0.55 MPa. The exploitation method of the #2 coal seam by the LW23209 working face is fully-mechanized mining; the mining height is 1.2 m, and the advance rate of working face is 3.6 m/d. Y type ventilation is used in LW23209 working face. The type of shearer, scraper conveyer, and hydraulic support are MG2 × 160/710 AWD, SGZ730/320, and ZY3600/07/15, respectively. The lower #3 coal seam, a protected coal seam with limited levels of gas permeability, presents the greatest outburst risks. Relative gas content and gas pressure levels from this coal seam reach 27.82 m^3/t and 2.03 MPa, respectively. The average interlayer space between the protected and protective coal seams covers 17.5 m. Main features of the stratum are shown in Table 1.

To eliminate coal and gas outburst risks in the #3 coal seam, the #2 coal seam is chosen as the protective seam. However, when multi-layered coal seams are present, stress-relieved gas from adjacent coal seams can trigger a gas explosion [13] (Yang et al., 2014). Therefore, measures should be taken to ensure safe mining in the protective seam to realize safe and efficient coal mining with gas extraction.

Table 1. The main attitude of the stratum.

S.N.	Lithological Characters	Thickness/m	Description
1	Fine sandstone	8.0	Gray, laminated, horizontal bedding, mixed with sheet mica, medium-level separation
2	Siltstone	3.0	Dark gray, mixed with cloud-type plant fossils
3	#2 upper coal seam	0.5	Black, lumpy, fragmentary, and granulous
4	Siltstone	3.5	Dark gray, with cloud-type plant fossils
5	Fine sandstone	4.0	Gray, partly mixed with plant fossils
6	#2 coal seam	1.0	Black, lumpy, fragmentary, and granulous
7	Argillaceous siltstone	2.5	Gray black, laminated, facially with plant fossils
8	Siltstone	5.0	Gray, argillaceous cemented, laminated, with plant leaf fossils on the face, tuber fossils in the upper part and fine sandstone in the middle.
9	Medium-fine sandstone	8.0	Gray, gray-white, silicon, argillaceous cemented, mainly mixed with quartz
10	Siltstone	2.0	Gray argillaceous cemented lump, with fracture development
11	#3 coal seam	6.0	Black, powder-type, scale-like, fragmentary, and granulous
12	Sandy mudstone	3.0	Gray black, gray, with plant fossil fragments and star mica
13	Fine sandstone	5.0	Gray, gray-white, with carbon dust and quantities of mica sheets on the front layer

3. Stress-Relief Effects of Protective Coal Seam Mining

Coal is a porous media that contains a large number of fractures and pores [31]. Under original stress levels, fractures are often small apertures that hinder the free flow of gas. However, such fractures can stretch, shear, or break as a result of changes in stress levels that occur during mining operations. When stress is released, fractures expand and thus form flow channels of gas, as shown in Figure 3. In the figure, σ_z is the vertical stress and σ_x is the horizontal stress. In other words, higher normal stress will shrink cracks, and lower normal stress will expand cracks. The expansion and shrinkage of cracks significantly affect the rock mass permeability and methane flow character [32].

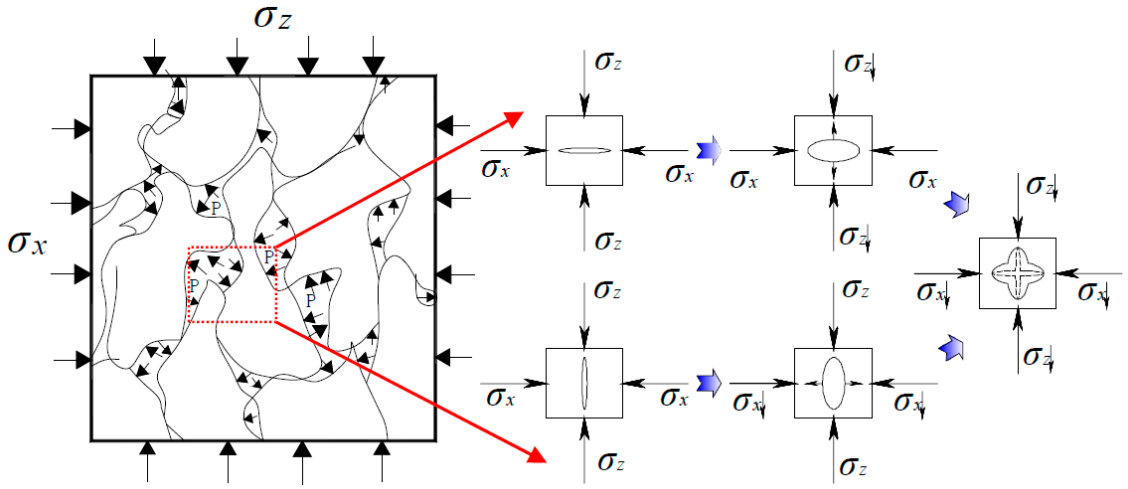

Figure 3. Relationship between pressure relief and fracture expansion.

Fractured rock masses generally have time-dependent properties. The failure mechanism of a protective coal seam floor is related to an increase in failure cracking and to the evolution of porosity features. Based on the hypothesis that any point can lose efficacy in a porous medium, failure development and porosity evolution in adjacent region media should occur immediately. Furthermore, with the intensification and spread of damage, the porosity of floor rock masses is improved, releasing stress off of the protected seam, enhancing gas permeability levels, and supporting efficient gas drainage.

According to Darcy's permeability law [33,34],

$$K = \mu_f \times \frac{l}{A} \times \frac{Q_f}{\Delta P} \tag{1}$$

where K is Darcy permeability, D; Q_f is the volume flow rate, cm^3/s; μ_f is gas viscosity, cp; A is the gross area of cross section flows, cm^2; ΔP is the pressure drop, atm; and l is the length of the pressure drop, cm. A coal seam is a typical porous medium of matrices and fractures [35], and Darcy permeability has an inverse relationship with pressure drop. As is shown in Figure 4, the stress relief mechanism of a mining protective coal seam can be illustrated as follows: as a gas outburst coal seam deforms, stress is released and permeability levels increase under the mining effects of protective coal seams; with the application of enhanced gas drainage, gas pressure and content generally drop to 0.6 MPa and to 50% or lower, respectively. Meanwhile, the consistence coefficient of the gas outburst coal seam increases to 48–100%. Consequently, the gas discharge level decreases considerably while driving and advancing; in turn, outburst risks among protected coal seams are eliminated.

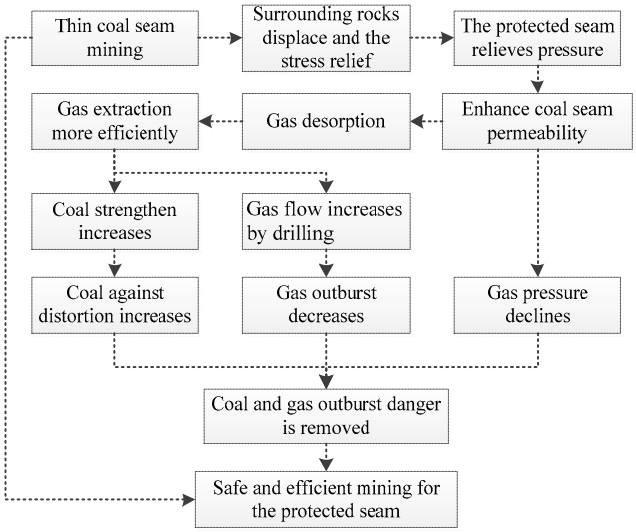

Figure 4. The protected seam stress relief induced by protective seam mining.

4. Gas Permeability Evolution Mechanism Accompanied by Protective Coal Seam Mining

4.1. Gas Permeability of the Rock and Its Calculation

The overburden strata above the mining seam can be divided into four vertical zones: caved zone, fractured zone, continuous deformation zone, and surface zone from the bottom to the top [36] (Zhang et al., 2016a). In this model, the permeability of the caved zone, fractured zone, and continuous deformation zone were important to the stress relief gas migration. The caved zone is made up of the crushed rock and coal and the porosity is up to 30–45% according to laboratory measurement [36]. The fractal permeability model was proposed by Karacan (2010) [37], this approach allowed the calculation of porosity and permeability from the size distribution of broken rock material in the goaf using flow and fractal crushing equations for granular materials. In this paper, the permeability of the caved zone can be calculated by Equation (2), with fitting from the stress permeability behaviour of the post failure rocks [38].

$$K_{g0} = -4 \times 10^{-16}\varepsilon_{\mathrm{vol}}{}^3 - 6 \times 10^{-15}\varepsilon_{\mathrm{vol}}{}^2 - 7 \times 10^{-14}\varepsilon_{\mathrm{vol}} + 10^{-11} \quad (2)$$

where $\varepsilon_{\mathrm{vol}}$ is the volumetric strain of the caved coal and rock in the gob. Whittles et al. (2006) provided the relationship among the bulk modulus K, shear modulus G, vertical stress σ_v, vertical strain ε, and maximum vertical strain ε_m, as expressed in Equation (3) [39]. Using this equation, the gradually compacting process of the caved zone rock can be simulated by using the FISH language with the updated parameters. Further, the permeability of the caved zone is updated according to Equation (2).

$$K = \frac{4G}{3} = \frac{\sigma_v}{2\varepsilon} = \frac{E_0}{2(1-\varepsilon/\varepsilon_m)} \quad (3)$$

The permeability of the fractured zone and continuous deformation zone can be measured by laboratory experiments. As for the relationship between the permeability of elastic rock and the stress in continuous deformation zone, Ren and Edwards (2002) determined the index relationship between permeability and stress [40]:

$$K_h = K_{h0} \times e^{-0.25(\sigma_{xx}-\sigma_{xx0})}, K_h = K_{h0} \times e^{-0.25(\sigma_{xx}-\sigma_{xx0})} \quad (4)$$

where K_h and K_v represent the permeability of the rock in the horizontal and vertical directions, respectively, m^2/Pa·s; K_{h0} and K_{v0} represent the initial permeability of the rock in the horizontal and vertical directions, respectively, m^2/Pa·s; σ_{yy} and σ_{xx} refer to the stress of the rock in the horizontal

and vertical directions, respectively, MPa; and σ_{yy0} and σ_{xx0} are the stress of original rock in the horizontal and vertical directions, respectively, MPa. According to the further studies by Durucan (1981) and Whittles et al. (2006) [39,41], the relationship between the permeability of the fractured rock and maximum/minimum principal stresses in the fractured zone is obtained from the laboratory results analysis:

$$K_f = K_{f0} \times \frac{(\sigma_1 + \sigma_3)}{2}^{0.816} \quad (5)$$

where K_f is the permeability of the fractured rock, $m^2/Pa{\cdot}s$, and σ_1 and σ_3 are the maximum and minimum principal stresses, respectively, MPa. K_{f0} is the permeability when $(\sigma_1 + \sigma_3)/2 = 1$ MPa, $m^2/Pa{\cdot}s$.

With the above equations, the elastic model is used for the caved zone and modified K according to Equation (3). The failure criteria of others rock stratum are defined by the Mohr-coulomb model. In order to verify the accuracy of the algorithm, it was used to simulate the uniaxial compression test, and the results are compared with the experimental data, as shown in Figure 5. In the figure, the numerical simulation results of the stress-strain and stress-permeability characteristics are in good agreement with those of the experimental data.

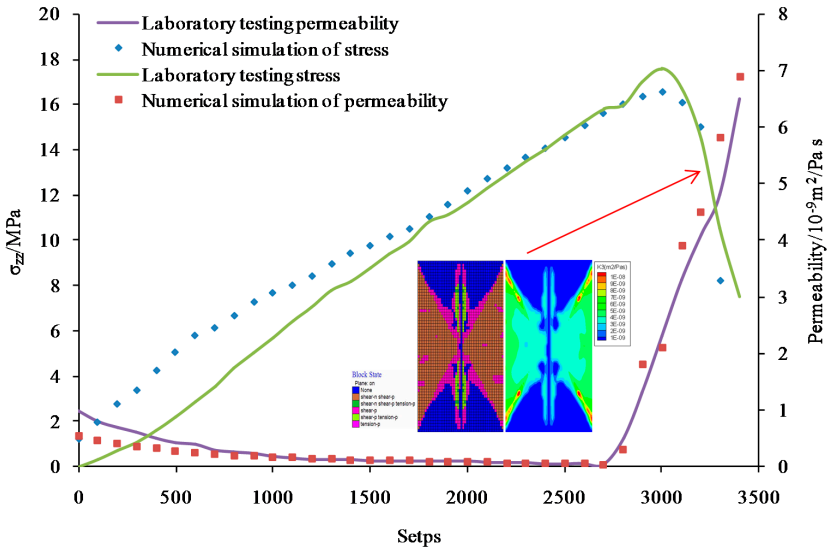

Figure 5. Modeling results of uniaxial compression and permeability-stress change curve.

4.2. Simulation Numerical Model Establishment

A numerical model was established based on the geological conditions of the LW23209 working face, as shown in Figure 6. Extensive simulations show that when the mined length of the longwall panel in numerical simulation is more than 100 m, the overburden movement and stress evolution law can well simulated [25,32]. Thus, in order to improve simulation efficiency, the length of the model is 300 m, its inclination length is 200 m, and its height is 80 m. Relative to the buried depth of the coal seam, 10 MPa of compressive stress is loaded averagely on the upper boundary of the model. Simulation parameters of the surrounding rock were determined through a laboratory test, as shown in Table 2. The parameters of the goaf in Table 2 are used to assign the initial parameters when the coal seam is mined out, and they are continually updated according to Equation (3) to simulate the process of caved zone compaction [42]. Based on Equations (2)–(5), a simple algorithm written in FISH language, an internal programming language available through FLAC3D (version 5.0, Itasca Consulting Group, Inc., Minneapolis, MI, USA) [43], is imported into the reservoir model. It is possible to calculate the permeability of each zone during mining with this algorithm [44,45]. Using the above model, gas seepage is simulated.

Table 2. Physical and mechanical parameters of rocks and coal.

S.N.	Lithology	Thickness/m	Density/kg·m^{-3}	Bulk Modulus/GPa	Shear Modulus/GPa	Cohesion/MPa	Internal Friction Angle/°	Tensile Strength/MPa
1	Overlying rock	20.0	2500	3.0	1.5	2.0	35	1.5
2	Silt sand layer	3.5	2500	2.6	1.6	2.2	36	1.5
3	Fine sandstone	4.0	2500	2.9	1.9	2.8	36	1.8
4	#2 coal seam	1.0	1450	1.8	1.0	1.5	39	1.0
5	Argillaceous silt sandstone	2.5	2300	2.0	1.3	2.0	38	1.5
6	Silt sandstone	5.0	2400	2.6	1.6	2.2	36	1.5
7	Medium-fine sandstone	8.0	2600	4.0	2.4	2.8	38	2.8
8	Fine sandstone	2.0	2400	2.6	1.6	2.2	36	1.5
9	#3 coal seam	6.0	1400	1.8	1	1.5	30	1.0
10	Sandy mudstone	3.0	2400	2.0	1.3	1.5	30	1.2
11	Fine sandstone	5.0	2500	2.8	1.8	2.9	36	1.7
12	Underlying rock layer	20.0	2500	3.0	1.5	2.0	35	1.5
13	Caved zone	4.2	1900	13.9	0.15	0.001	5	0

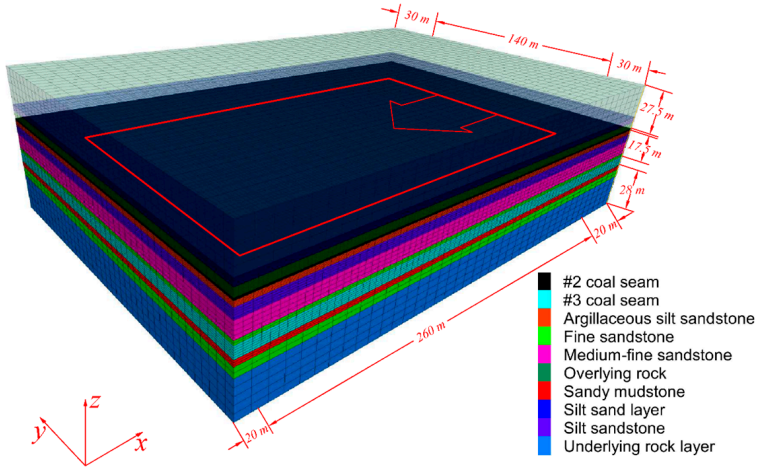

Figure 6. Numerical simulation model.

4.3. Evolution of Gas Permeability

During the initial mining phase (the first 50 m) of the model, advances occur once every 5 m; thereafter, advances occur once every 10 m until mining is completed. The evolution of permeability is simulated using the FISH language embedded in FLAC3D, and the corresponding simulation results are shown in Figures 7 and 8. In the figure, the unit of permeability is $m^2/(Pa \cdot s)$, and 1 mD is equal to 9.036×10^{-11} $m^2/(Pa \cdot s)$.

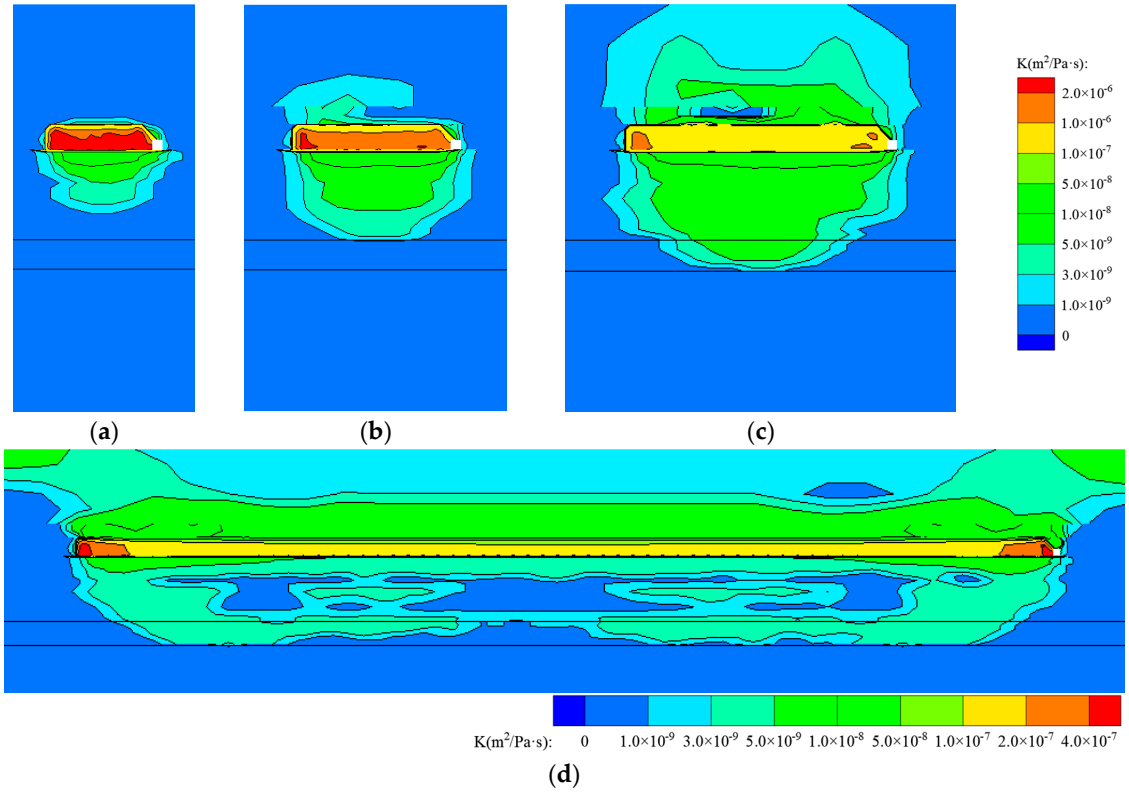

Figure 7. Vertical permeability contour of coal seam and rock with different cumulative advancing lengths; (**a**–**d**) 20 m, 30 m, 50 m, and 260 m respectively.

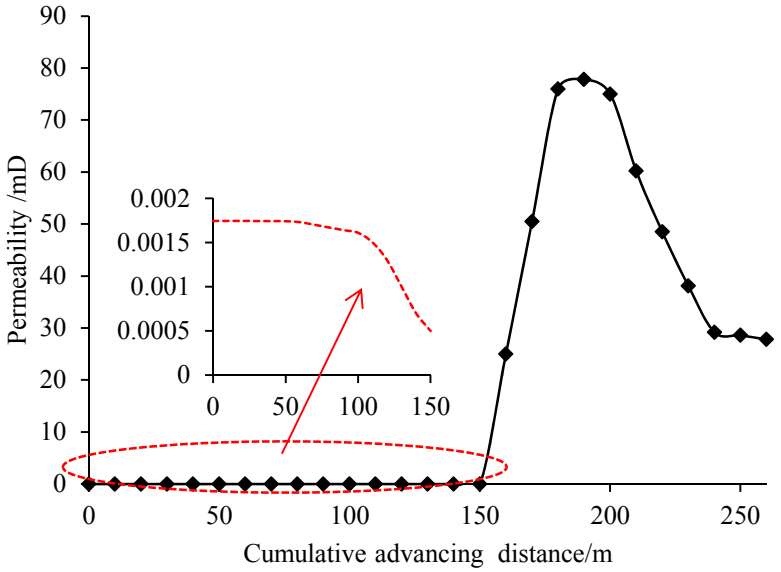

Figure 8. Gas permeability evolution curves of the protected coal seam from the start-line (0 m) to 260 m.

Figure 7 shows that protective seam mining will cause a substantial increase in the permeability of the protected seam and of the stratum in between. Permeability levels will increase with the advancement of the working face, and the permeability enhancement area will expand to the protected seam. When the advancing distance reaches 50 m, this area will be positioned close to the floor of the protected coal seam, meaning that protective seam mining has a remarkable effect on adjacent coal seams. To further determine how the permeability of the protected seam evolves during protective seam mining, a monitor point is set in the middle of the protected seam at a 150-m horizontal distance from the set-up entry of the protective seam. Figure 8 shows the permeability evolution of the protected seam during a 260 m advancing process. Before the working face of the protective seam advances to the monitor point, the permeability of the protected seam decreases slowly from 0.001745 mD to 0.0005 mD, mainly because protective seam mining has caused the accumulation of abutment stress in the floor. When the working face passes the monitor point, it enters the stress-relief zone and causes the permeability of the protected seam to increase dramatically from 0.0005 to 77.8 mD. Thereafter, due to the compaction of the goaf, the protected seam permeability level gradually declines and finally stabilizes at 27.0 mD. However, the permeability is still significantly higher than the initial value, showing that protective seam mining has clear effects in terms of relieving stress and increasing permeability in the protected seam.

4.4. Gas Seepage Characteristics

Based on our numerical simulation on permeability evolution, gas seepage calculations were simulated. The gas pressure levels of the protected and protective seams are 2.03 MPa and 0.55 MPa, respectively. To reduce calculation times, the indirect fluent-solid coupling operation method was used for the simulation, and the corresponding results are shown in Figures 9 and 10.

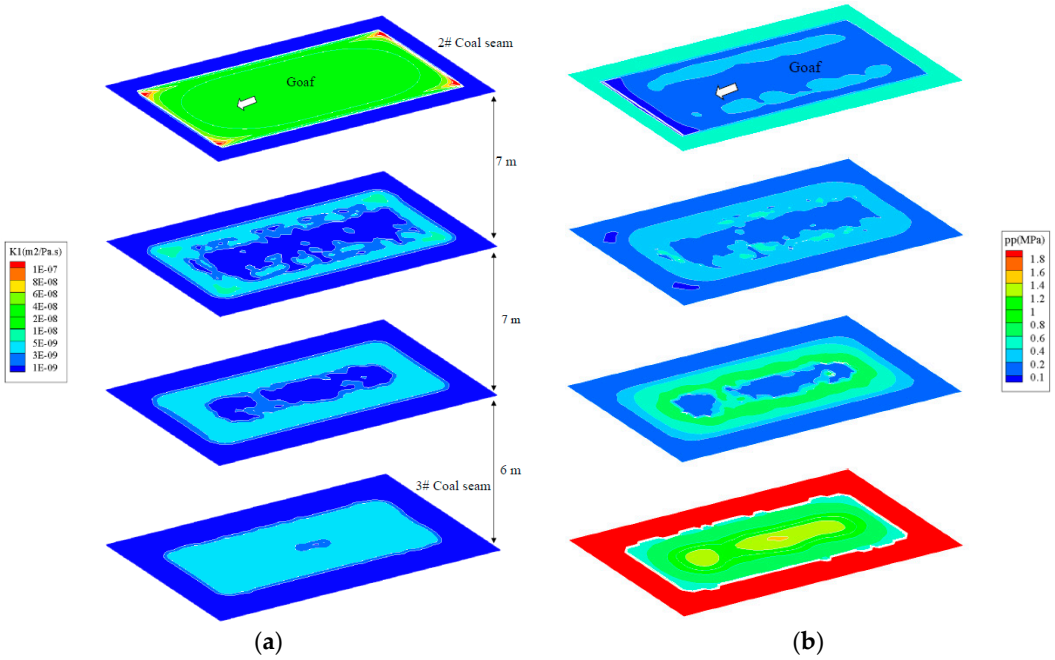

Figure 9. Cross-sectional diagram of gas permeability and gas pressure in different layer spacing between the protective seam and protected seam; (**a**) gas permeability, and (**b**) gas pressure.

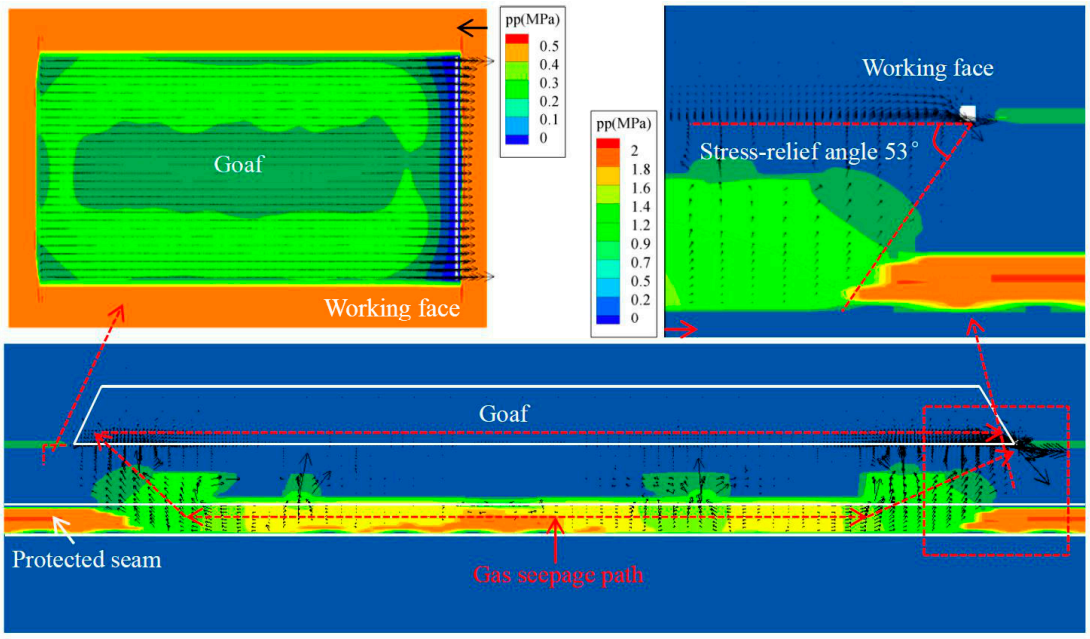

Figure 10. Gas seepage path during the mining process.

As shown in Figure 9, the maximum permeability level progressively decreases with distance from the protective seam. However, the range of permeability increase found in the coal seam is greater than that found in the rock. This suggests that the native coal seam fracture is relatively more developed and exhibits higher levels of permeability increase with stress relief. Meanwhile, stress-relief gas flows along the permeability increasing area from the protected seam to the goaf and longwall face. As the degree of permeability range increase of the coal seam is greater than that of the rock, a large amount of stress-relief gas remains in the rock mass between the protective seam and protected seam, as shown in Figure 9b. Moreover, due to goaf compaction, the inner-region permeability of

the rock mass under the goaf is relatively low, resulting in a less significant reduction of gas pressure in the central area of the protected seam. Thus, comprehensive gas drainage technologies must be applied to further reduce stress-relief gas levels in the protected seam and in the rock mass between the protective seam and protected seam. Figure 10 shows that stress-relief gas from the protected seam mainly flows along the two ends of the goaf towards the working face. This can easily cause gas to exceed the limit in the working face of the protective seam. Thus, gas monitoring should be enhanced, and gas drainage holes should be drilled through the floor of the goaf area to ensure safe production. Figure 10 also shows that the seepage path, goaf area, and protected seam are major gas sources and that gas drainage holes should be arranged for gas extraction. In conclusion, goaf-side roadway retention and high-position extraction through the roof are used for goaf gas drainage. Gas drainage hole drilling through the protected seam was applied to drain gas from the protected seam, and drainage holes were arranged within the stress-relief angle of the protective seam, i.e., within the main gas seepage path.

5. Analysis of Comprehensive Gas Drainage Technologies and their Effects

5.1. Comprehensive Gas Drainage Technologies for Stress-Relief Gas

To prevent the gas pressure level from exceeding the limit in the LW23209 working face and to prevent an outburst in the #3 coal seam, comprehensive gas extraction technologies for stress-relief gas were used. This approach is designed to capture stress relief gas and to reduce the gas content and gas pressure levels of the protected seam. The comprehensive extraction tool proposed in this paper involves the stress-relief extraction of the goaf-side entryway floor, retaining high-position extraction through roof fractures, high-position extraction with large diameter long holes through the roof, gas extraction in the goaf area, and strengthening the ventilation system. The gas extraction pipelining path and the positions of drilling holes in the LW23209 working face are shown in Figure 11.

(1) Floor stress-relief extraction for goaf-side roadway retention (FSRE)

To extract stress-relief gas from the protected seam, gas drainage holes are drilled through the protected seam of the goaf-side roadway. Drainage holes are drilled 5 m away from the set-up entry every 5 m alongside the working face in the direction of the goaf-side roadway. Gas extraction is carried out through a 250 m^3/min extraction pump positioned on the ground, and the extraction angle of the borehole is set to 30°, which will cross #3 coal seam with a borehole depth of 45 m, as shown in Figure 11.

(2) High-position gas extraction through roof fractures (HPGE)

A 3 × 3 × 3 m extraction drilling site was built 50 m away from the set-up entry every 50 m alongside the working face in the direction of goaf-side roadway. Every drilling site includes nine gas drainage holes positioned close to the set-up entry in the direction of the goaf-side roadway. Through these drainage holes, gas in the goaf and in the upper corner of the working face can be extracted. The boreholes are designed as shown in Figure 11.

(3) High-position extraction by large-diameter long holes through roof fractures (HPELDLH)

Two special extraction drilling sites for drainage holes are included in the LW23209 working face. One is located along the goaf-side roadway 400 m away from the set-up entry, and the other lies along the connection roadway. Every drilling site includes 11 gas drainage holes with ends positioned 10–15 m above the set-up entry (or the working face). These drainage holes are used to capture gas in the roof fissure zone. The borehole designs are shown in Figure 11.

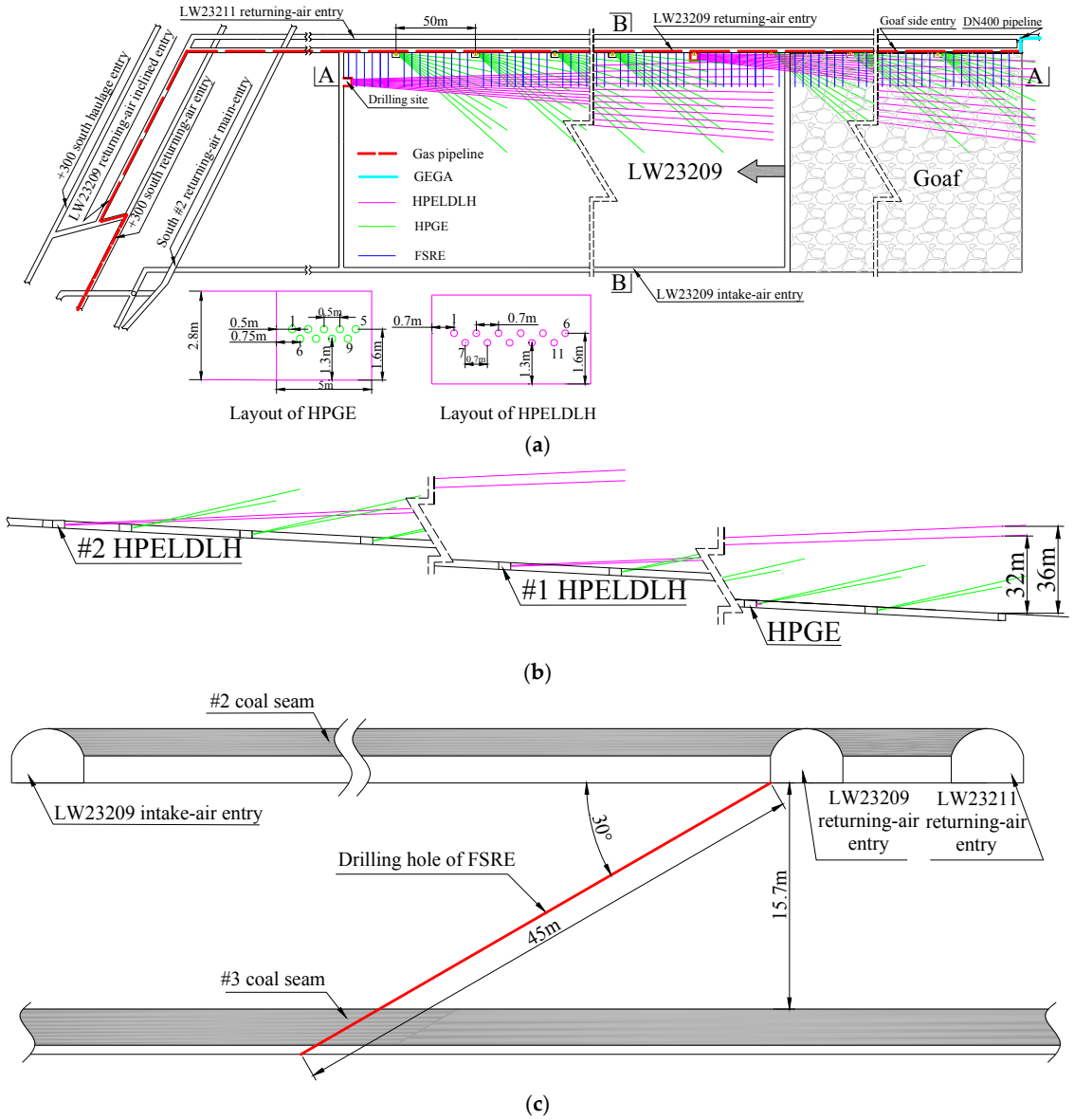

Figure 11. Gas drainage pipelines and borehole layout: (**a**) Pipelines and borehole layout; (**b**) Section A-A; (**c**) Section B-B.

(4) Gas extraction in the goaf area (GEGA) (HPELDLH)

Before mining the LW23209 working face, the original returning-air entry of the 23,211 working face was closed through a connection entry in the LW23209 working face. Meanwhile, a DN400 type extraction pipeline was positioned within the goaf of the LW23209 working face to extract gas in the goaf during LW23209 working face mining.

(5) Strengthening the ventilation system

The ventilation system of the working face was adjusted from a "U" type ventilation configuration to a "Y" type ventilation system (a more reliable ventilation system for the working face) via goaf-side roadway retention.

5.2. Comprehensive Gas Drainage Effect Evaluation

Statistics obtained from field measurements, gas extraction volumes, and ventilation air methane levels of the LW23209 working face are shown in Figures 12 and 13.

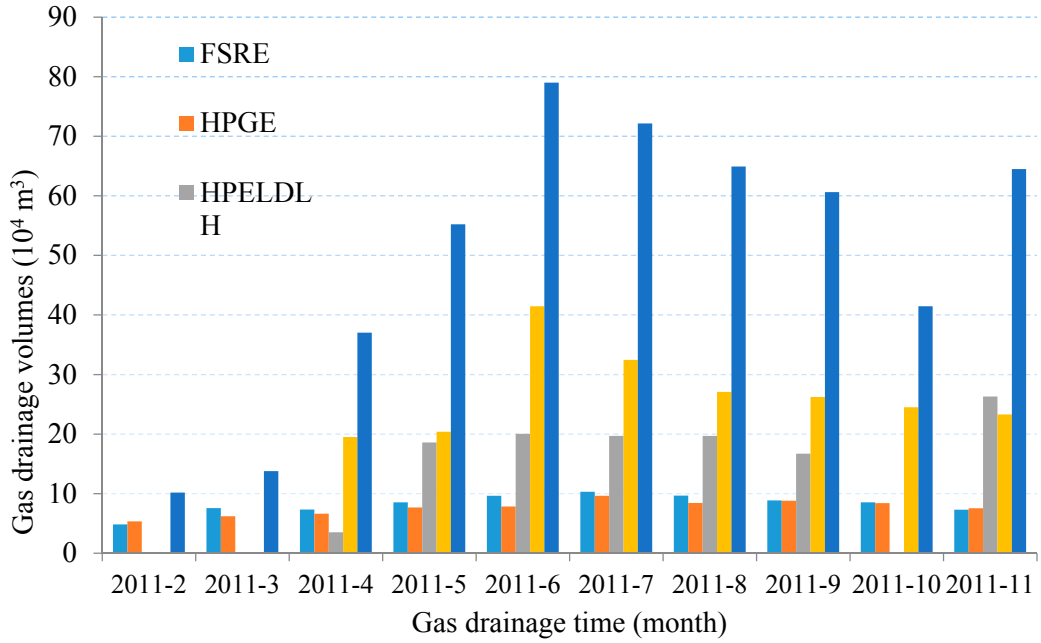

Figure 12. Gas drainage statistics.

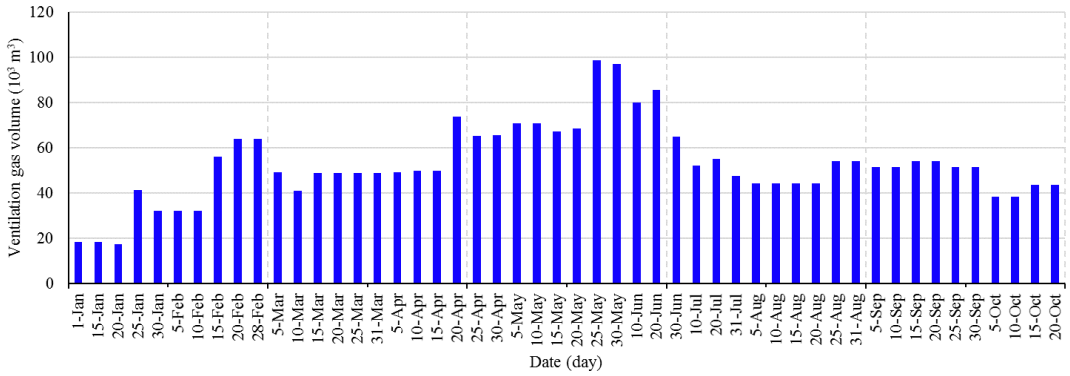

Figure 13. Ventilation gas volume statistics.

Figures 12 and 13 show that gas extraction occurred from February 2011 to June 2011. During this period, gas extraction volume gradually increased to 0.7899 million m^3/month. This is especially true for high-position extraction from large-diameter long holes through roof fractures and the goaf area, mainly because the constant mining-induced scope expansion of the working face leads to a synchronous augmentation of gas accumulation in the goaf and roof. Consequently, gas content in the working face slightly decreased, and gas extraction volumes and ventilation air methane levels followed the same trend, indicating that stress-relief gas extraction has had a significant effect.

With the application of comprehensive extraction technologies in protective seam mining, gas content and pressure in the protected seam declined considerably prior to the start of mining operations. The maximum gas content and residual gas pressure were measured after protective coal seam mining, and their levels reached 6.45 m^3/t and 0.62 MPa, respectively. These two parameters fall below

controlled gas content (8 m^3/t) and gas pressure (0.74 MPa) levels, indicating a good prevention of coal and gas outbursts.

6. Conclusions

Stress relief gas extraction technology has been successfully implemented and has been regarded as a coal seam gas exploitation and outburst prevention technology. The main requirement of this technology is to find an appropriate coal seam as a protective coal seam and ensure that the protected coal seam is included in the desorption zone to enhance its permeability. In addition, the gas seepage path and the distribution of gas pressure is important to the location of the gas extraction borehole. In this paper, using FLAC3D, and taking into account specific geological conditions for a particular case of longwall panel in Hancheng coal mine in Shaanxi Province, as well as the permeability changes of the surrounding rock in the mining process of the protective seam, the distribution of permeability in the protected seam and goaf is obtained. On this basis, the gas flow characteristics could be easily reflected by the change of rock mass permeability. This provides reasonable extraction time and location for the comprehensive gas extraction technology.

The stress relief mechanism of protective coal seam mining can be summarized as follows: the gas-outburst coal seam deforms; stress is released and permeability increases with protective coal seam mining effects, involving enhanced gas drainage; and gas pressure and content levels of the protected coal seam generally drop from 2.03 MPa and 27.82 m^3/t to 0.62 MPa and 6.45 m^3/t, respectively. Meanwhile, the methane consistency in the gas extraction of the gas-outburst coal seam increases by 48–100%. Consequently, the degree of gas extraction decreases observably while the working face drives and advances, eliminating outburst risks within the protected coal seam.

The numerical simulation results also indicate that protective seam mining will contribute to a substantial increase in the permeability of the protected seam and of the rock layer in between. The protected seam permeability level gradually declines with goaf compaction and finally stabilizes at 27.0 mD. However, permeability levels are still significantly higher than the initial value, meaning that protective seam mining has a clear effect on protected seam stress relief and permeability increase effects. The gas seepage simulation results show that stress-relief gas from the protected seam mainly flows along the two ends of the goaf towards the working face. This flow can easily cause gas levels to exceed limits in the working face of the protective seam.

To prevent gas levels from exceeding the limit in the LW23209 working face and to prevent the outburst of the #3 coal seam, comprehensive gas extraction technologies for stress-relief gas were applied. The comprehensive extraction technologies proposed in this study involve extraction through the goaf-side roadway retaining floor, high-position extraction through roof fractures, high-position extraction through the use of long, large-diameter holes drilled through the roof, gas extraction in the goaf area, and strengthening the ventilation system. By applying comprehensive extraction technologies to processes of protective seam mining, protected seam gas content and gas pressure levels declined more significantly than ever before. Maximum gas content and residual gas pressure levels reached 6.45 m^3/t and 0.62 MPa, respectively, and thus fell below the controlled gas content and gas pressure limits necessary for the prevention of coal and gas outburst disasters. Thin coal seam mining applied to form a protective layer in upper coal and gas outburst prone coal seams thus has significant effects in terms of relieving stress and increasing permeability levels. When thin coal seam mining is integrated with comprehensive gas drainage technologies, safe, efficient, and eco-friendly mining can be realized.

Acknowledgments: Fundamental Research Funds for the Central Universities (2014XT01) and Priority Academic Program Development of Jiangsu Higher Education Institutions (PAPD).

Author Contributions: Comprehensive gas drainage technology in stress relief mining was proposed by Fangtian Wang and he also analyzed the gas permeability evolution mechanism during stress relief mining; Numerical simulation with FLAC3D of the stress relief mining was carried out by Cun Zhang and Ningning Liang provided field measured data during the revision of the article.

Conflicts of Interest: The authors declare no conflict of interest.

References

1. Xie, H.P.; Zhou, H.W.; Xue, D.J.; Gao, F. Theory, technology and engineering of simultaneous exploitation of coal and gas in China. *J. China Coal Soc.* **2014**, *39*, 1391–1397.
2. Wang, L.; Cheng, Y.P.; Xu, C.; An, F.H.; Jin, K.; Zhang, X.L. The controlling effect of thick-hard igneous rock on pressure relief gas drainage and dynamic disasters in outburst coal seams. *Nat. Hazards* **2013**, *66*, 1221–1241. [CrossRef]
3. Wang, H.; Cheng, Y.; Yuan, L. Gas outburst disasters and the mining technology of key protective seam in coal seam group in the Huainan coalfield. *Nat. Hazards* **2013**, *67*, 763–782. [CrossRef]
4. Wang, H.; Cheng, Y.; Wang, W.; Xu, R. Research on comprehensive CBM extraction technology and its applications in China's coal mines. *J. Nat. Gas Sci. Eng.* **2014**, *20*, 200–207. [CrossRef]
5. Liu, Q.; Cheng, Y. Measurement of pressure drop in drainage boreholes and its effects on the performance of coal seam gas extraction: A case study in the Jiulishan Mine with strong coal and gas outburst dangers. *Nat. Hazards* **2014**, *71*, 1475–1493. [CrossRef]
6. Xu, T.; Tang, C.A.; Yang, T.H.; Zhu, W.C.; Liu, J. Numerical investigation of coal and gas outbursts in underground collieries. *Int. J. Rock Mech. Min. Sci.* **2009**, *43*, 905–919. [CrossRef]
7. Xu, C.; Cheng, Y.; Ren, T.; Wang, L.; Kong, S.; Lu, S. Gas ejection accident analysis in bed splitting under igneous sills and the associated control technologies: A case study in the Yangliu Mine, Huaibei Coalfield, China. *Nat. Hazards* **2014**, *71*, 109–134. [CrossRef]
8. Li, Q.; Lin, B.; Zhai, C. A new technique for preventing and controlling coal and gas outburst hazard with pulse hydraulic fracturing: A case study in Yuwu coal mine, China. *Nat. Hazards* **2015**, *75*, 2931–2946. [CrossRef]
9. Meng, Y.; Li, Z.; Lai, F. Experimental study on porosity and permeability of anthracite coal under different stresses. *J. Pet. Sci. Eng.* **2015**, *133*, 810–817. [CrossRef]
10. Yuan, L. Gas distribution of the mined-out side and extraction technology of first mined key seam relief-mining in gassy multi-seams of low permeability. *J. China Coal Soc.* **2008**, *33*, 1362–1367.
11. Yuan, L. Theory of pressure-relieved gas extraction and technique system of integrated coal production and gas extraction. *J. China Coal Soc.* **2009**, *34*, 1–8.
12. Zhou, F.B.; Wang, X.X.; Liu, Y.K. Gas drainage efficiency: An input-output model for evaluating gas drainage projects. *Nat. Hazards* **2014**, *74*, 989–1005. [CrossRef]
13. Yang, W.; Lin, B.Q.; Yan, Q.; Zhai, C. Stress redistribution of longwall mining stope and gas control of multi-layer coal seams. *Int. J. Rock Mech. Min. Sci.* **2014**, *72*, 8–15. [CrossRef]
14. Yang, W.; Lin, B.Q.; Xu, J.T. Gas outburst affected by original rock stress direction. *Nat. Hazards* **2014**, *72*, 1063–1074. [CrossRef]
15. Somerton, W.H.; Söylemezoglu, I.M.; Dudley, R.C. Effect of stress on permeability of coal. *Int. J. Rock Mech. Min. Sci. Geomech.* **1975**, *12*, 129–145. [CrossRef]
16. McKee, C.R.; Bumb, A.C.; Koenig, R.A. Stress-dependent permeability and porosity of coal and other geologic formations. *SPE Form. Eval.* **1988**, *3*, 81–91. [CrossRef]
17. Enever, J.R.E.; Henning, A. The relationship between permeability and effective stress for Australian coal and its implications with respect to coalbed methane exploration and reservoir model. In Proceedings of the International Coalbed Methane Symposium, University of Alabama, Tuscaloosa, AL, USA, 12–17 May 1997; Volume 22.
18. Guo, H.; Yuan, L.; Shen, B.; Qu, Q.; Xue, J. Mining-induced strata stress changes, fractures and gas flow dynamics in multi-seam longwall mining. *Int. J. Rock Mech. Min. Sci.* **2012**, *54*, 129–139. [CrossRef]
19. Hungerford, F.; Ren, T.; Naj, A. Evolution and application of in-seam drilling for gas drainage. *Int. J. Min. Sci. Technol.* **2013**, *23*, 543–553.
20. Hungerford, F.; Ren, T. Directional drilling in unstable environments. *Int. J. Min. Sci. Technol.* **2014**, *24*, 397–402. [CrossRef]

21. Jiang, J.Y.; Cheng, Y.P.; Wang, L.; Li, W.; Wang, L. Petrographic and geochemical effects of sill intrusions on coal and their implications for gas outbursts in the Wolonghu Mine, Huaibei Coalfield, China. *Int. J. Coal Geol.* **2011**, *88*, 55–66. [CrossRef]
22. Li, D.; Li, H. A new technology for the drilling of long boreholes for gas drainage in a soft coal seam. *J. Pet. Sci. Eng.* **2015**, *137*, 107–112. [CrossRef]
23. Wang, F.T.; Ren, T.; Tu, S.H.; Hungerford, F.; Aziz, N. Implementation of underground longhole directional drilling technology for greenhouse gas mitigation in Chinese coal mines. *Int. J. Greenh. Gas Control* **2012**, *11*, 290–303. [CrossRef]
24. Wang, L.; Cheng, Y.P.; An, F.H.; Zhou, H.X.; Kong, S.L.; Wang, W. Characteristics of gas disaster in the Huaibei coalfield and its control and development technologies. *Nat. Hazards* **2014**, *71*, 85–107. [CrossRef]
25. Karacan, C.Ö.; Diamond, W.P.; Schatzel, S.J.; Garcia, F. Development and application of reservoir models for the evaluation and optimization of longwall methane control systems. In Proceedings of the 11th US/North American Mine Ventilation Symposium, University Park, PA, USA, 5–7 June 2006; pp. 425–432.
26. Schatzel, S.J.; Karacan, C.Ö.; Dougherty, H.; Goodman, G.V. An analysis of reservoir conditions and responses in longwall panel overburden during mining and its effect on gob gas well performance. *Eng. Geol.* **2012**, *127*, 65–74. [CrossRef]
27. Jia, J.; Cao, L.; Sang, S.; Yi, T.; Zhou, X. A case study on the effective stimulation techniques practiced in the superposed gas reservoirs of coal-bearing series with multiple thin coal seams in Guizhou, China. *J. Pet. Sci. Eng.* **2016**, *146*, 489–504. [CrossRef]
28. Zhang, C.; Tu, S.H.; Bai, Q.S.; Yang, G.Y.; Zhang, L. Evaluating pressure-relief mining performances based on surface gas venthole extraction data in longwall coal mines. *J. Nat. Gas Sci. Eng.* **2015**, *24*, 431–440. [CrossRef]
29. Li, D. Mining thin sub-layer as self-protective coal seam to reduce the danger of coal and gas outburst. *Nat. Hazards* **2014**, *71*, 41–52. [CrossRef]
30. Zhao, T.; Zhang, Z.; Tan, Y.; Shi, C.; Wei, P.; Li, Q. An innovative approach to thin coal seam mining of complex geological conditions by pressure regulation. *Int. J. Rock Mech. Min. Sci.* **2014**, *71*, 249–257. [CrossRef]
31. Zhang, Z.; Jan, N.; Ren, T.; Zhang, J. Influence of void space on microscopic behavior of fluid flow in rock joints. *Int. J. Min. Sci. Technol.* **2014**, *24*, 335–340. [CrossRef]
32. Yang, W.; Lin, B.; Qu, Y.; Zhao, S.; Zhai, C.; Jia, L.; Zhao, W. Mechanism of strata deformation under protective seam and its application for relieved methane control. *Int. J. Coal Geol.* **2011**, *85*, 300–306. [CrossRef]
33. Bear, J. Dynamics of fluids in porous media. *Soil Sci.* **1972**, *120*, 174–175. [CrossRef]
34. Fu, X.H.; Qin, Y.; Wang, G.G.X.; Rudolph, V. Evaluation of coal structure and permeability with the aid of geophysical logging technology. *Fuel* **2009**, *88*, 2278–2285. [CrossRef]
35. Packham, R.; Cinar, Y.; Moreby, R. Simulation of an enhanced gas recovery field trial for coal mine gas management. *Int. J. Coal Geol.* **2011**, *85*, 247–256. [CrossRef]
36. Zhang, C.; Tu, S.; Chen, M.; Zhang, L. Pressure-relief and methane production performance of pressure relief gas extraction technology in the longwall mining. *J. Geophys. Eng.* **2017**, *14*, 77–89. [CrossRef]
37. Karacan, C.Ö. Prediction of porosity and permeability of caved zone in longwall gobs. *Transp. Porous Med.* **2010**, *82*, 413–439. [CrossRef]
38. Jozefowicz, R.R. The Post-Failure Stress-Permeability Behaviour of Coal Measure Rocks. Ph.D. Thesis, University of Nottingham, Nottingham, UK, 1997.
39. Whittles, D.N.; Lowndesa, I.S.; Kingmana, S.W.; Yates, C.; Jobling, S. Influence of geotechnical factors on gas flow experienced in a UK longwall coal mine panel. *Int. J. Rock Mech. Min. Sci.* **2006**, *43*, 369–387. [CrossRef]
40. Ren, T.X.; Edwards, J.S. Goaf gas modeling techniques to maximize methane capture from surface gob wells. In *Mine Ventilation*; De Sauza, E., Ed.; Swets and Zeitlinger B.V.: Lisse, The Netherlands, 2002; pp. 279–286.
41. Durucan, S. An Investigation into the Stress-Permeability Relationship of Coals and Flow Patterns around Working Longwall Faces. Ph.D. Thesis, University of Nottingham, Nottingham, UK, 1981.
42. Yavuz, H. An estimation method for cover pressure re-establishment distance and pressure distribution in the goaf of longwall coal mines. *Int. J. Rock Mech. Min. Sci.* **2004**, *41*, 193–205. [CrossRef]
43. Itasca Consulting Group, Inc. *FLAC3D User's Guide*; Itasca Consulting Group, Inc.: Minneapolis, MN, USA, 2011.

44. Zhang, C.; Tu, S.; Zhang, L.; Wang, F.; Bai, Q.; Tu, H. The numerical simulation of permeability rules in protective seam mining. *Int. J. Oil Gas Coal Technol.* **2016**, *13*, 243–259. [CrossRef]
45. Zhang, C.; Tu, S.; Zhang, L.; Bai, Q.; Yuan, Y.; Wang, F. A methodology for determining the evolution law of gob permeability and its distributions in longwall coal mines. *J. Geophys. Eng.* **2016**, *13*, 181–193. [CrossRef]